Supporting Information

Crystallographic, Spectroscopic, and Computational Characterization of a Diiodonaphthoquinone Diarylethene Photochrome: Halogen Bonding and Photocrystallography

Shea D. Myers [a,†], Zoe Y. Marr[a,†], Jade A. Sency[b], Travis B. Mitchell,[a] Jason B. Benedict[a,] and Dinesh G. Patel[b,*]*

*dgp15@psu.edu

*jbb6@buffalo.edu

[a] Department of Chemistry, University at Buffalo, Buffalo NY 14228
[b] Department of Chemistry, The Pennsylvania State University, Hazleton PA 18202
[†] both authors contributed equally to this work

Table of Contents

Figure S1. Absorption spectra of compounds **1a** and **1b** in methylene chloride (9.6 x 10^{-5} M). **S2**

Figure S2. Time resolved UV-Vis spectra of a solution of compounds **1a** and **1b** upon irradiation with 430 nm light (9.6 x 10^{-5} M solution in methylene chloride) **S3**

Figure S3. Time resolved UV-Vis spectra of a solution of compounds **1a** and **1b** upon irradiation with 623 nm light (9.6 x 10^{-5} M solution in methylene chloride) **S4**

Figure S4. Solid-state UV-vis spectrum of a microcrystalline thin film (thickness 5.5 μm) of **1b**. **S4**

Figure S5: Images illustrating the molecular orbitals associated with the three lowest energy electronic transitions with oscillator strength greater than 0.1 for **XB-dimer**. **S5**

Table S1: Electronic transitions and orbital contributions for the calculated UV-vis spectra of **1a**, **1b**, and **XB-dimer**. **S6**

Table S2. First eight electronic transitions with oscillator strengths greater than 0.01 for **1a**, **1b**, and **XB-dimer**. **S7**

Table S3. Crystallographic information for **1b** and **1b-irradiated**. **S8**

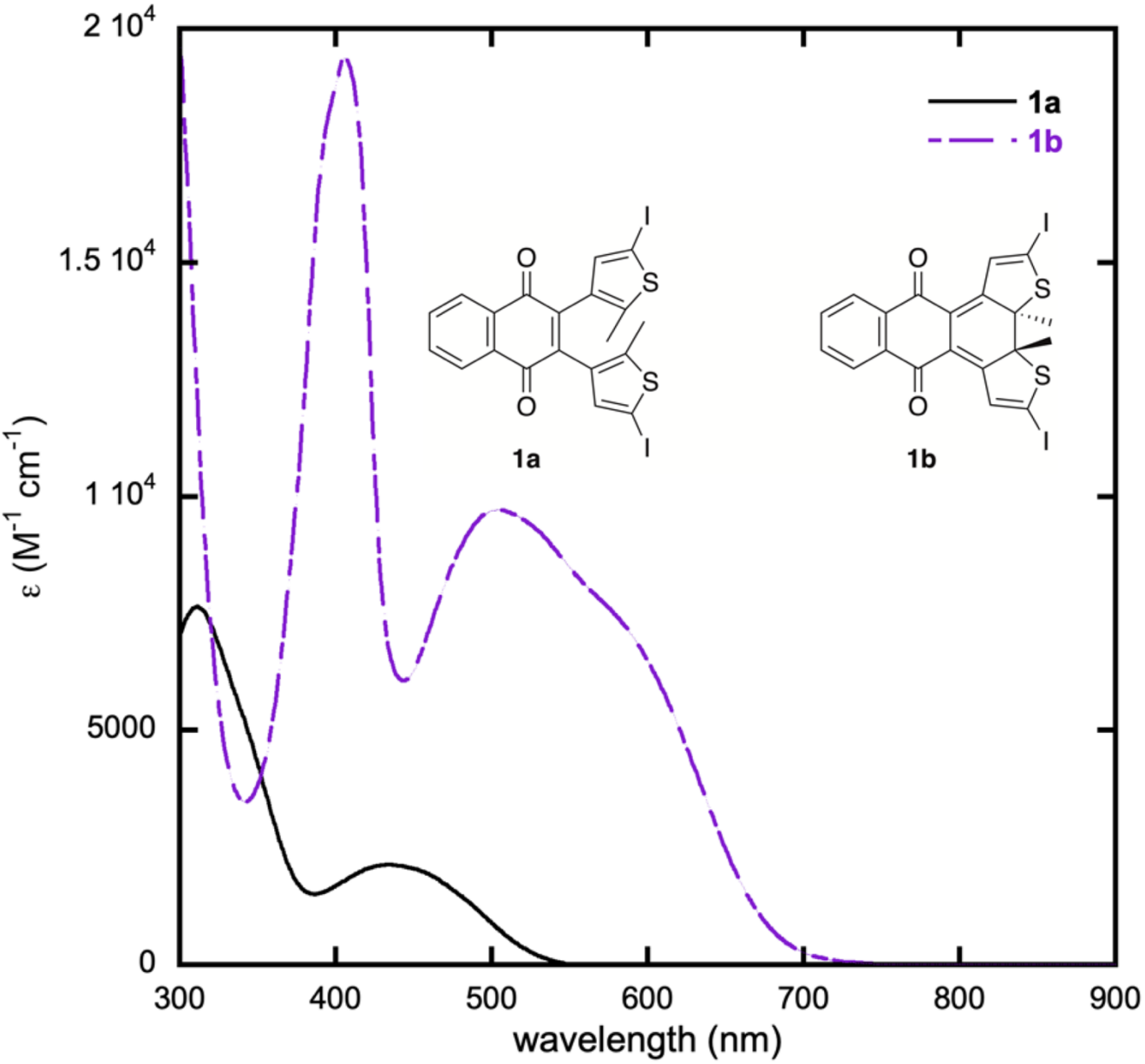

Figure S1. Absorption spectra of compounds **1a** and **1b** in methylene chloride (9.6×10^{-5} M).

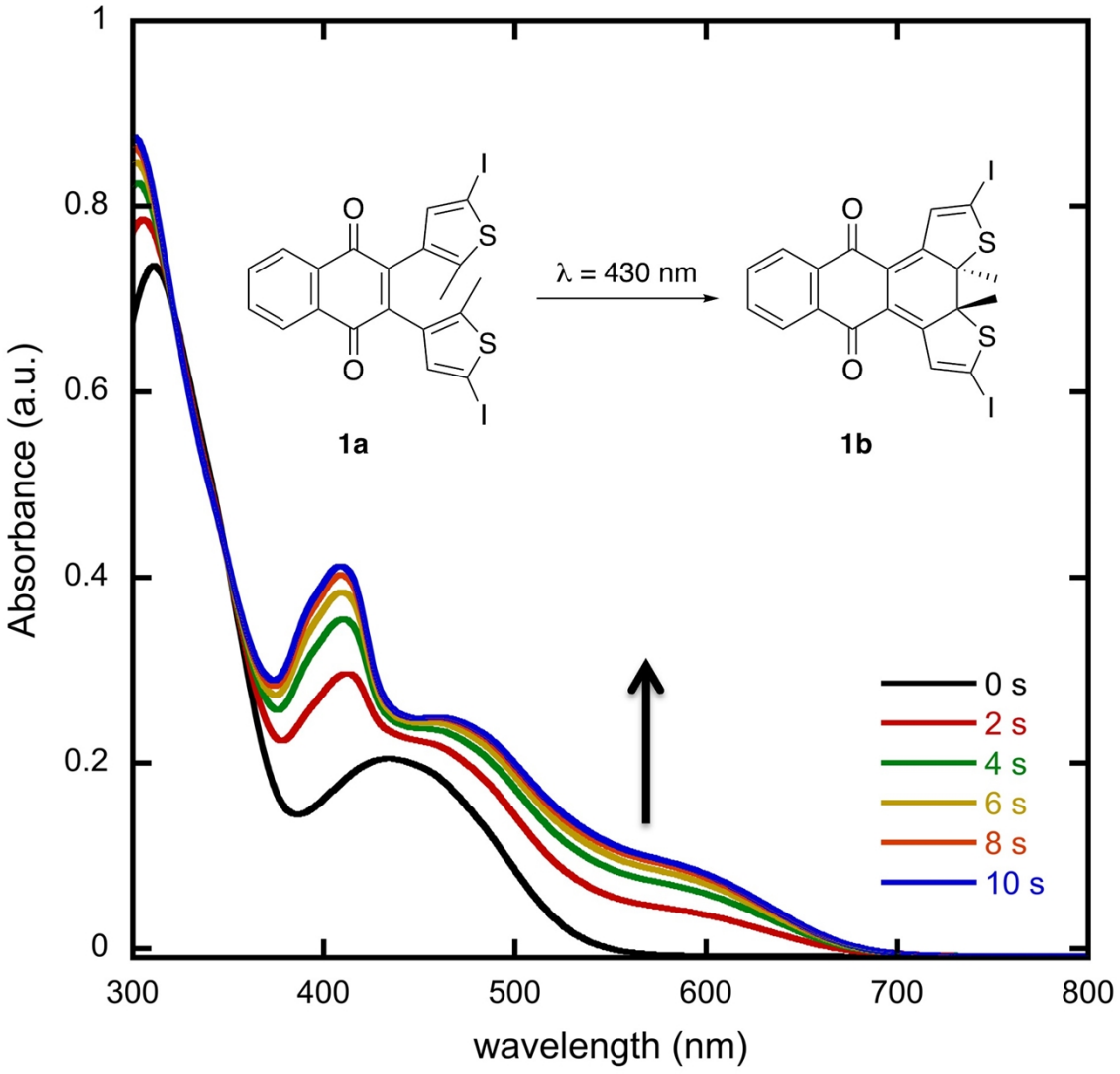

Figure S2. Time resolved UV-Vis spectra of a solution of compounds **1a** and **1b** upon irradiation with 430 nm light (9.6 x 10^{-5} M solution in methylene chloride).

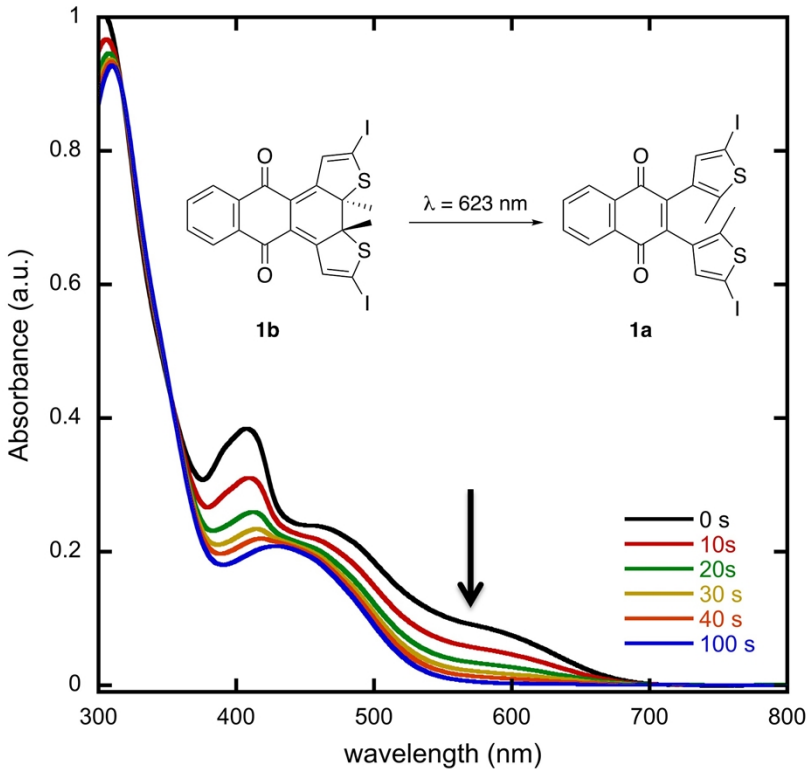

Figure S3. Time resolved UV-Vis spectra of a solution of compounds **1a** and **1b** upon irradiation with 623 nm light (9.6 x 10^{-5} M solution in methylene chloride).

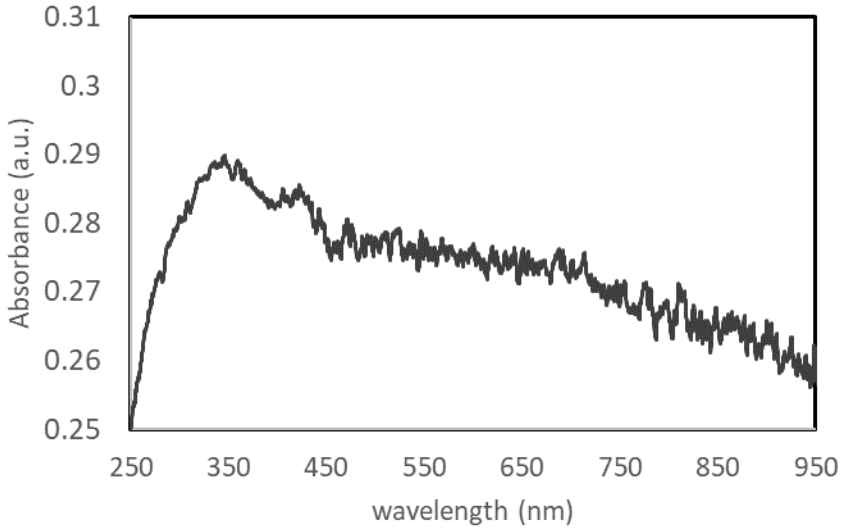

Figure S4. Solid-state UV-vis spectrum of a microcrystalline thin film (thickness 5.5 μm) of **1b**.

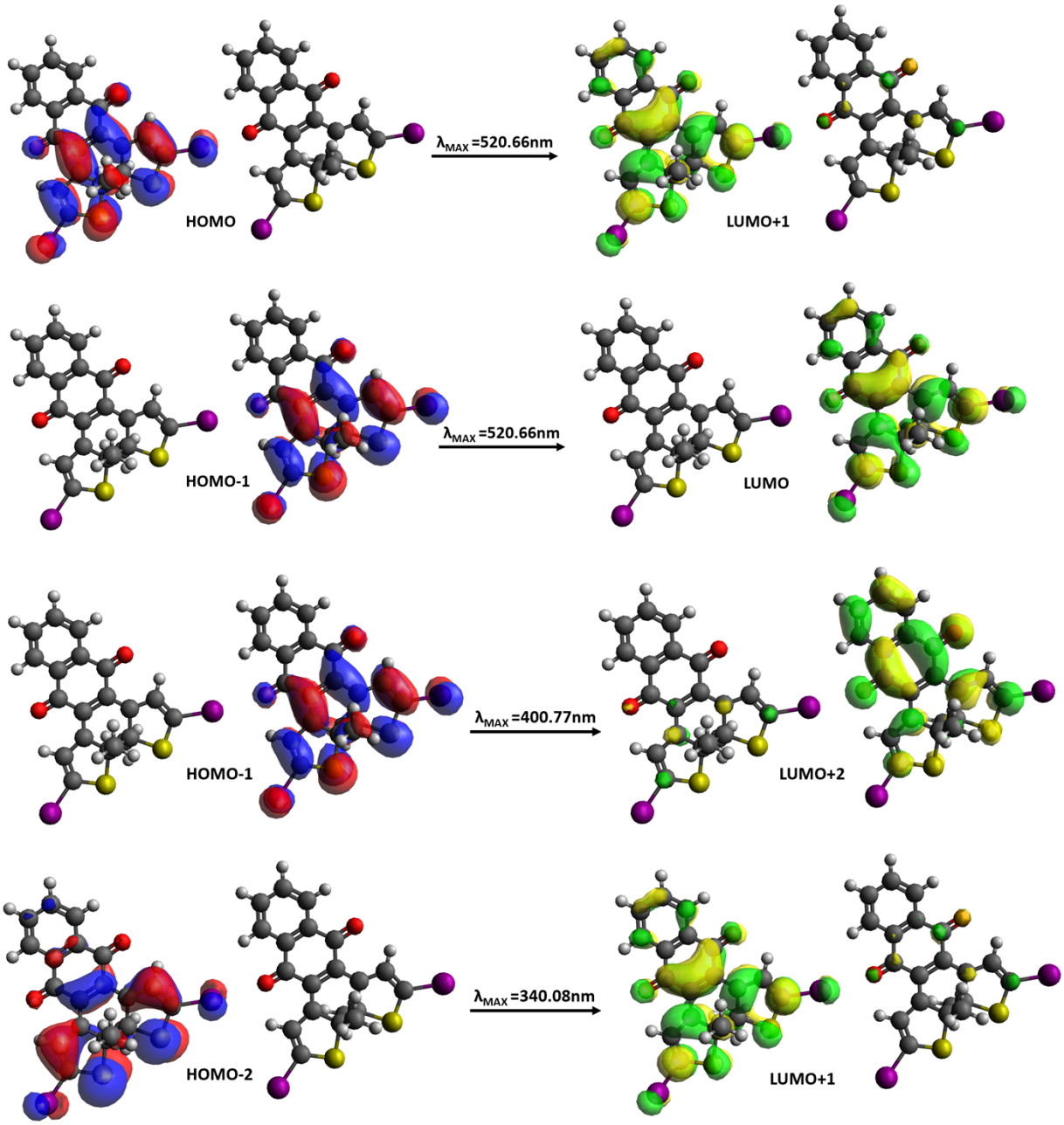

Figure S5: Images illustrating the molecular orbitals associated with the three lowest energy electronic transitions with oscillator strength greater than 0.1 for **XB-dimer**.

Table S1: Electronic transitions and orbital contributions for the calculated UV-vis spectra of **1a**, **1b**, and **XB-dimer**.

Molecule	Transition	Excited state	Singlet-A
1A	427.55 nm	106→116 (HOMO-9→LUMO) 107→116 (HOMO-8→LUMO) 108→116 (HOMO-7→LUMO) 111→116 (HOMO-4→LUMO) 115→116 (HOMO→LUMO)	0.12761 (3.2569%) -0.39152 (30.658%) 0.15848 (5.0232%) -0.12168 (2.9612%) 0.50228 (50.457%)
1A	405.81 nm	104→117 (HOMO-11→LUMO+1) 106→116 (HOMO-9→LUMO) 107→116 (HOMO-8→LUMO) 111→116 (HOMO-4→LUMO) 113→116 (HOMO-2→LUMO) 115→116 (HOMO→LUMO)	0.10086 (2.0354%) -0.21621 (9.3494%) 0.36955 (27.313%) 0.11118 (2.4722%) -0.23653 (11.189%) 0.45114 (40.705%)
1A	318.00 nm	106→116 (HOMO-9→LUMO) 108→116 (HOMO-7→LUMO) 113→116 (HOMO-2→LUMO) 115→116 (HOMO→LUMO)	-0.10104 (2.0418%) -0.17762 (6.3098%) 0.63414 (80.427%) 0.15345 (4.7094%)
1A	283.17 nm	105→116 (HOMO-10→LUMO) 109→116 (HOMO-6→LUMO) 112→116 (HOMO-3→LUMO)	-0.12514 (3.1320%) 0.17176 (2.9501%) 0.63822 (81.465%)
1B	500.02 nm	115→116 (HOMO→LUMO)	0.69716 (97.206%)
1B	382.27 nm	106→117 (HOMO-9→LUMO+1) 115→117 (HOMO→LUMO+1)	-0.16453 (5.4140%) 0.66390 (88.153%)
1B	327.70 nm	105→117 (HOMO-10→LUMO+1) 106→117 (HOMO-9→LUMO+1) 110→116 (HOMO-5→ LUMO) 114→116 (HOMO-1→LUMO)	0.14425 (4.16161%) -0.15038 (4.5228%) -0.17576 (6.17832%) 0.61850 (76.508%)
XB-dimer	520.66 nm	229→231 (HOMO-1→LUMO) 230→232 (HOMO→LUMO+1)	0.52634 (55.407%) 0.44203 (39.078%)
XB-dimer	400.77 nm	229→232 (HOMO-1→LUMO+1) 229→233 (HOMO-1→LUMO+2) 230→234 (HOMO→LUMO+3)	0.17796 (6.3339%) 0.62390 (77.850%) -0.16481 (5.4325%)
XB-dimer	340.08 nm	210→234 (HOMO-20→LUMO+3) 223→232 (HOMO-7→LUMO+1) 228→232 (HOMO-2→LUMO+1) 230→233 (HOMO→LUMO+2)	0.13874 (3.8498%) 0.10656 (2.2710%) 0.62873 (79.060%) -0.14465 (4.1847%)

Table S2. First eight electronic transitions with oscillator strengths greater than 0.01 for **1a**, **1b**, and **XB-dimer**.

f>0.01	Species	**DAE-NQ-I (1a)**	**DAE-NQ-I-c (1b)**	**XB-dimer**
Transition 1	λ (nm)	427.55	500.02	520.66
	f	0.0155	0.1413	0.3058
Transition 2	λ (nm)	405.81	382.28	400.77
	f	0.0302	0.2685	0.4720
Transition 3	λ (nm)	325.00	360.91	398.48
	f	0.0138	0.1212	0.1535
Transition 4	λ (nm)	318.00	327.70	372.89
	f	0.0359	0.1419	0.0296
Transition 5	λ (nm)	283.17	263.20	362.98
	f	0.0785	0.0144	0.0576
Transition 6	λ (nm)	281.26	258.60	356.19
	f	0.0621	0.0795	0.0542
Transition 7	λ (nm)	272.30	256.38	340.94
	f	0.0863	0.1012	0.0840
Transition 8	λ (nm)	248.04	253.10	340.08
	f	0.0896	0.0189	0.1216

Table S3. Crystallographic information for **1b** and **1b-irradiated**.

Identification code	**1b**	**1b-irradiated**
Empirical formula	$C_{20}H_{12}I_2O_2S_2$	$C_{20}H_{12}I_2O_2S_2$
Formula weight	602.22	602.22
Temperature/K	298	298
Crystal system	monoclinic	monoclinic
Space group	$P2_1$	$P2_1$
a/Å	11.9319(10)	11.911(4)
b/Å	7.4644(6)	7.520(3)
c/Å	12.4586(10)	12.479(5)
α/°	90	90
β/°	117.024(2)	117.134(9)
γ/°	90	90
Volume/Å^3	988.47(14)	994.7(7)
Z	2	2
ρ_{calc}g/cm^3	2.023	2.011
μ/mm^{-1}	3.405	3.383
F(000)	572.0	572.0
Crystal size/mm^3	0.5 × 0.25 × 0.15	0.4 × 0.1 × 0.05
Radiation	MoKα (λ = 0.71073)	MoKα (λ = 0.71073)
2Θ range for data collection/°	3.67 to 67.31	3.842 to 53.6

Index ranges	-18 ≤ h ≤ 18, -11 ≤ k ≤ 11, -19 ≤ l ≤ 19	-15 ≤ h ≤ 14, -9 ≤ k ≤ 8, -12 ≤ l ≤ 15
Reflections collected	26911	7591
Independent reflections	7775 [R_{int} = 0.0517, R_{sigma} = 0.0602]	3542 [R_{int} = 0.0711, R_{sigma} = 0.1034]
Data/restraints/parameters	7775/1/238	3542/1/241
Goodness-of-fit on F^2	1.106	0.990
Final R indexes [I>=2σ (I)]	R_1 = 0.0432, wR_2 = 0.1184	R_1 = 0.0520, wR_2 = 0.1111
Final R indexes [all data]	R_1 = 0.0768, wR_2 = 0.1317	R_1 = 0.1261, wR_2 = 0.1358
Largest diff. peak/hole / e $Å^{-3}$	1.90/-1.46	0.99/-0.78
Flack parameter	0.47(6)	0.37(17)